Surface Hopping Dynamics with DFT Excited States[†]

Mario Barbatti[1*] and Rachel Crespo-Otero[2]

[1]*Max-Planck-Institut für Kohlenforschung,*
Kaiser-Wilhelm-Platz 1, D-45470 Mülheim an der Ruhr, Germany
[2] *Department of Chemistry, University of Bath,*
Claverton Down, BA2 7AY - Bath, United Kingdom

[*]*Electronic address: barbatti@kofo.mpg.de*

Abstract

Nonadiabatic dynamics simulation of electronically-excited states has been a research area of fundamental importance, providing support for spectroscopy, explaining photoinduced processes, and predicting new phenomena in a variety of specialties, from basic physical-chemistry, through molecular biology, to materials engineering. The demands in the field, however, are quickly growing, and the development of surface hopping based on density functional theory (SH/DFT) has been a major advance in the field. In this contribution, the surface hopping approach, the methods for computation of excited states based on DFT, the conection between these methodolgies, and their diverse implementations are reviewed. The shortcomings of the methods are critically addressed and a number of case studies from diverse fields are surveyed.

Keywords

Surface Hopping, Density Functional Theory, Excited States, Nonadiabatic Dynamics, Photochemistry

---

[†] Cite this work as: Mario Barbatti and Rachel Crespo-Otero, Top. Curr. Chem., doi: 10.1007/128_2014_605 (2015).

Abbreviations

ADC	Algebraic diagrammatic construction
ALDA	Adiabatic local density approximation
CASSCF	Complete active space self-consistent field
CC	Coupled cluster
CI	Configuration interaction
CIS	CI with single excitations
CPA	Classical path approximation
DFT	Density functional theory
DFTB	Density functional based tight binding
DISH	Decoherence-induced surface hopping
GFSH	Global-flux surface hopping
LR	Linear response
KS	Kohn-Sham
MCSCF	Multiconfigurational self-consistent field
MRCI	Multireference CI
MR-CISD	MRCI with singles and doubles
MRPT	Multireference perturbation theory
REKS	Spin-restricted ensemble-referenced KS
ROKS	Restricted open-shell KS
RPA	Random phase approximation
SDKS	Single determinant KS
SH	Surface hopping
SH/DFT	Surface hopping with DFT excited states
TD	Time-dependent
TDA	Tamm-Dancoff approximation
TDHF	Time-dependent Hartree-Fock
UBS	Spin-unrestricted broken symmetry

1 Introduction

Motivated by the advances in computational capabilities and algorithms, computational research on dynamics simulations of electronically-excited molecular systems has been quickly developing in the last decade. Larger and more complex systems are reported from groups all over the world on a daily basis, providing fundamental information to interpret excited-state phenomena revealed by advanced spectroscopic techniques, to explain the photochemical process occurring in different fields, and to predict new properties with potential technological applications.

There are a relatively large number of methods for excited-state calculations available. They include wavefunction-based and density-functional-based methods derived from different approaches, as configuration interaction, perturbation theory, and coupled cluster; and resting on different approximation levels, from semiempirical to fully first principles, from single-reference to multireference, from short truncated spaces to complete configurational expansions. Each of these methods and their hybrid combinations has its own domain of applicability depending on the nature and size of the molecular system. Exactly for this reason, none of them can be expected to perform equally well for every problem without exception.

Extensive benchmarks of excitation energies have shown that most of methods present mean deviation errors of about 0.2-0.3 eV for vertical excitation energies [1-5]. Not only such values are of the order of magnitude of many reaction barriers, but these errors are unevenly distributed among several states for the same method and tend to grow bigger out of the Franck-Condon region. Well known examples are the relatively large errors on the energy of ionic states predicted by truncated *ab-initio* configuration interaction [6] or on the energy of charge-transfer states of time-dependent density functional theory with conventional functionals [7].

The root of this problem rests on the very nature of the electronic excitations. Electronically-excited states lie close to each other in the energy spectrum and relatively small variations in the molecular geometry may lead to their reordering. Moreover, the character of these states may be extremely different: from diffuse Rydberg, through charge-transfer, to spatially localized densities.

Given those features, a basic requirement for a proper computational description of an excited-state phenomenon is that the theoretical model should describe different types of states for different nuclear geometries on the same footing. At this moment, this is a requirement that no single method can fully and affordably satisfy. The consequence is that the simulations often deliver an unbalanced description of the electronic states, with deep implications on the reliability of predictions.

This problem is under relative control in static simulation of reaction pathways, where only few degrees of freedom are considered. In dynamics simulations, however, it may grow out of control due to the much larger number of degrees of freedom and variables (now, time among them) to tackle.

Besides the question of the accuracy of the potential energy surfaces, dynamics simulations add two new layers of potential complications to the simulations: first, nonadiabatic phenomena [8-9], originated by the coupling of nuclear and electronic degrees of freedom during the dynamics propagation, must be taken into account; second, the dynamics propagation itself multiplies the computational costs.

Again, several methods are available for nonadiabatic excited-state dynamics simulations, from full propagation of the electronic wavefunctions [10], which requires predefinition of multidimensional potential energy surfaces, to semiclassical approximations, which reduce the wavefunction propagation to ensembles of independent trajectories based only on local properties [11]. In particular, the independent-trajectory approximation, essential to the surface hopping approach, cannot predict nonlocal quantum effects, such as tunneling, quantum phases, or decoherence [8, 12-13]. Moreover, the statistical ensembles are often of too reduced size to comply with the computational capabilities, leading to high statistical uncertainties [14]. (For recent discussions on nonadiabatic dynamics beyond the independent-trajectories approach, see Refs. [15-17].)

From the point of view of semiclassical nonadiabatic excited-state dynamics simulations, the ideal method for electronic structure calculations should satisfy the following criteria:

1. Be computationally fast.
2. Provide energies for excited states of different natures with similar accuracy.
3. Provide reliable (preferentially analytical) gradients for excited states.
4. Allow the computation of electronic structures near intersection seams with the ground state.
5. Allow the computation of electronic structures near intersection seams between excited states.
6. Be independent of human intervention for running large ensembles of different geometries.

With different accuracies, methods for excited-states computation based on DFT comply with most of these criteria, especially computational efficiency. These methods, however, usually fail for criterion 4, the description of the crossing seam with the ground state. Nevertheless, still considering the *pros* and *cons*, surface hopping based on DFT excitations (SH/DFT) is a good alternative for nonadiabatic simulations, under the condition that it is applied critically, bearing in mind all these restrictions and limitations.

In this contribution, we will exam the current situation of the SH/DFT methods, starting by a review of the surface hopping in Section 2. In Section 3, we will address the methods for computing excited state in the DFT framework, specially focusing on the linear-response time-dependent methodology and its relation to lower-level methods (Section 3.1). In Section 3.2, we will review the computation of nonadiabatic couplings in DFT. In Section 3.3, the limitations of the method in the context of dynamics simulations are critically addressed. In Section 4, the elements from Sections 2 and 3 will be put together to discuss the different SH/DFT implementations. Finally, in Section 5, we will present a series of case studies showing the potentials and limitations of using SH/DFT in diverse fields.

2 Surface hopping overview

In surface hopping, the time propagation of the quantum wavepacket is approximated by a swarm of semiclassical trajectories evolving on Born-Oppenheimer surfaces of multiple electronic states. Nonadiabatic events (wavepacket density transfer between states; see Ref. [8] for an excellent review on this topic) are simulated by a stochastic algorithm that allows each trajectory to jump to other states during the propagation. Thus, the statistics over the ensemble of trajectories in terms of fraction of trajectories in each electronic state in each time step is expected to be an approximated representation of the wavepacket density distribution among the excited states as a function of time. The method was conceptually proposed by Nikitin [18] and had its earliest implementations done by Tully and Preston [19]. It has been recently reviewed in Refs. [11, 20-22].

In the most common surface hopping approach, all nuclear coordinates are driven by Newton's equations of motion on a single adiabatic electronic state *K*. For the coordinates $\mathbf{R}_m$ with the associated nuclear mass M_m, they are given by

$$\frac{d^2\mathbf{R}_m}{dt^2} = -\frac{1}{M_m}\frac{\partial E_K}{\partial \mathbf{R}_m}, \tag{1}$$

where E_K is the adiabatic potential energy of the current state *K*. Given a set of initial positions and velocities, Equation (1) is numerically integrated.

Simultaneously to the Newton's equations, the probability for the system to hop to another state *L* is evaluated. Diverse schemes for evaluation of such probabilities have been developed [19, 23-30]. The most successful and popular approach has been the fewest switches proposed by Tully in the early 1990's [28].

In the fewest switches, the number of hopping events within one time step Δt is minimized. Under this condition, the hopping probability between states K and L is

$$P_{K\to L} = \frac{\text{Population increment in } L \text{ due to flux from } K \text{ during } \Delta t}{\text{Population of } K}. \tag{2}$$

The population of each electronic state L is given in terms of the coefficients $c_L(t)$ of the time-dependent wavefunction written as a linear combination of electronic time-independent electronic wavefunctions Ψ_L:

$$\varphi(\mathbf{r},\mathbf{R},t) = \sum_J c_J(t)\Psi_J(\mathbf{r};\mathbf{R}(t)). \tag{3}$$

The coefficients c_J are obtained by solving a local approximation for the time-dependent electronic Schrödinger equation, given in the adiabatic representation by [28]

$$\frac{dc_L}{dt} + \frac{i}{\hbar}E_L c_L + \sum_J \sigma_{LJ}\, c_J = 0. \tag{4}$$

In this equation, the coupling terms between any pair of states L and M are

$$\sigma_{LM} \equiv \left\langle \Psi_L \middle| \frac{\partial}{\partial t}\Psi_M \right\rangle = \boldsymbol{\tau}_{LM}\cdot\mathbf{v} \tag{5}$$

where $\boldsymbol{\tau}_{LM}$ is the first-order nonadiabatic coupling vector

$$\boldsymbol{\tau}_{LM} \equiv \left\langle \Psi_L \middle| \nabla_{\mathbf{R}}\Psi_M \right\rangle. \tag{6}$$

and $\mathbf{v}$ is a vector collecting the nuclear velocities.

When explicit nonadiabatic coupling vectors $\boldsymbol{\tau}_{LM}$ are not available (and this is often the case for excited states based on DFT), the coupling terms σ_{LM} can be computed by finite differences as [31]

$$\begin{aligned}\sigma_{LM}(t) &\approx \frac{1}{2\Delta t}\left[\left\langle \Psi_L\left(t-\frac{\Delta t}{2}\right)\middle|\Psi_M\left(t+\frac{\Delta t}{2}\right)\right\rangle - \left\langle \Psi_L\left(t+\frac{\Delta t}{2}\right)\middle|\Psi_M\left(t-\frac{\Delta t}{2}\right)\right\rangle\right] \\ &\approx \frac{1}{4\Delta t}\left[3\mathrm{S}_{LM}(t) - 3\mathrm{S}_{ML}(t) - \mathrm{S}_{LM}(t-\Delta t) + \mathrm{S}_{ML}(t-\Delta t)\right],\end{aligned} \tag{7}$$

where $\mathrm{S}_{LM}(t) \equiv \left\langle \Psi_L(t-\Delta t)\middle|\Psi_M(t)\right\rangle$ are wavefunction overlaps between different time steps. This method can be generally used for any electronic-structure method, provided that a configuration interaction representation of the electronic wavefunction can be worked out [32-35]. In the last part of Eq. (7), the coupling is conveniently written in terms of full time steps (t, $t - \Delta t$, $t - 2\Delta t$) rather than in terms of midpoints ($t + \Delta t/2$, $t - \Delta t/2$) as done in the original model. This shift is explained in Ref. [33]. Comparisons between couplings computed with the finite-difference approach and with analytical derivatives are done in Refs. [33, 35-36].

Alternatively, c_L can still be obtained by the local diabatization approach [37]. In this case, instead of integrating Eq. (4), the array of coefficients after one time step is given by

$$\mathbf{c}\left(t+\Delta t\right) = \mathbf{T}^{-1}\exp\left(-\mathrm{i}\hbar^{-1}\frac{\mathbf{E}\left(t\right)+\mathbf{TE}\left(t+\Delta t\right)\mathbf{T}^{-1}}{2}\Delta t\right)\mathbf{c}\left(t\right), \tag{8}$$

where $\mathbf{E}$ is a diagonal matrix containing the adiabatic energies and $\mathbf{T}$ is an adiabatic-to-diabatic transformation constructed by a Löwdin orthogonalization of the $\mathbf{S}\left(t\right)$ wavefunction overlap matrix:

$$S_{LM}\left(t\right) = \sum_J \left\langle \eta_L\left(t-\Delta t\right) \middle| \eta_J\left(t\right)\right\rangle T_{JM}\left(t\right). \tag{9}$$

In this equation, $\{\left|\eta\right\rangle\}$ represents the diabatic basis, which is obtained along the trajectory as explained in Ref. [37]. It has been shown that this method is more stable in the presence of weak nonadiabatic couplings than conventional algorithms [38]. An alternative surface-hopping diabatization method is discussed in Ref. [39].

Either via Eq. (4) or (8), as soon as the coefficients c_L are obtained, the hopping probability can be computed and within the fewest switches approach in the adiabatic representation it is given by

$$P_{K\to L} = \max\left[0, \frac{-2\Delta t}{\left|c_K\right|^2}\mathrm{Re}\left(c_K c_L^*\right)\sigma_{LK}\right], \tag{10}$$

In the most recent implementations of the fewest switches, the coefficients c_L are corrected for decoherence effects [8, 40-42] before probabilities are computed [43-44].

Recently, Jaeger, Fischer, and Prezhdo proposed the decoherence-induced surface hopping (DISH) method, a hopping algorithm that relies entirely on the decoherence times of each adiabatic state to determine the state branching [30]. Another recently proposed alternative to the fewest switches is the global-flux surface hopping (GFSH) [23], which computes the hopping probability between groups of states with reduced or increased population. In this way, hops can occur even between non-directly coupled states (super-exchange).

Having the hopping probabilities at a time t, a stochastic algorithm is invoked to decide in which state the dynamics will continue in the next time step. A hopping from state K to state L occurs if a uniformly selected random number r_t in the [0, 1] interval is such that

$$\sum_{J=1}^{L-1} P_{K\to J}\left(t\right) < r_t \le \sum_{J=1}^{L} P_{K\to J}\left(t\right) \tag{11}$$

and the energy gap between the final and initial states satisfies [22]

$$E_L\left(\mathbf{R}\right) - E_K\left(\mathbf{R}\right) \le E_{kin}. \tag{12}$$

Eq. (12) ensures that if the nuclear kinetic energy (E_{kin}) cannot compensate the variation of potential energy, the hop is rejected ("frustrated hop"). If the state changes, the momentum is changed accordingly to ensure conservation of total energy. Normally, the momentum adjustment is done in the direction of the nonadiabatic coupling vector. When the vector direction is not available, as it is the case of computation of the coupling terms via Eq. (7), then the adjustment may be done along the linear momentum direction.

Surface hopping is not restricted to internal conversion and other types of nonadiabatic transitions may be considered, as those induced by spin-orbit couplings (intersystem crossing) [45-46] or electromagnetic fields [47-50]. From a general standpoint, to consider these effects it is enough to redefine the coupling term in Eq. (5). For instance, a σ_{KL} including simultaneously internal conversion, intersystem crossing, and an electromagnetic field may look like

$$\sigma_{LM} \equiv \left\langle \Psi_L \left| \frac{\partial}{\partial t} \Psi_M \right\rangle \right. - \frac{i}{\hbar} H_{LM}^{SO} - \frac{E_M - E_L}{\hbar^2 c} \boldsymbol{\mu}_{ML} \cdot \mathbf{A}_0 e^{-i\omega t}, \tag{13}$$

where H_{LM}^{SO} are the spin orbit couplings [46] and the last term accounts for the dipole interaction of the molecule with the field ($\boldsymbol{\mu}_{ML}$ is the transition dipole moment between the L and M) [49]. In section 3.2, we will discuss how these couplings can be computed within the DFT framework.

3 Excited states in DFT

3.1 Excitation energies in DFT

In this section, different approximations for the computation of excited states based on DFT are analyzed. We start from a general description of the popular linear-response (LR) TDDFT. A number of other methods for computing excitation energies based on DFT have been used for surface hopping as well. They will also be described here, highlighting the hierarchic relations between them. Methods alternative to linear response–like real-time TDDFT [51-52]–or beyond linear response [53] can be also used to study excited states, but their discussion are out of the scope of this paper, as these methods have not been generally applied for surface hopping so far. Multiconfigurational DFT is briefly addressed in Section 3.3.

The excitation energies ω_L in the LR-TDDFT are given by [54]

$$\mathbf{\Omega}\vec{F}_L = \omega_L^2 \vec{F}_L, \tag{14}$$

where

$$\mathbf{\Omega} = \left(\mathbf{A}-\mathbf{B}\right)^{1/2}\left(\mathbf{A}+\mathbf{B}\right)\left(\mathbf{A}-\mathbf{B}\right)^{1/2} \tag{15}$$

and the elements of **A** and **B** are

$$A_{ia,jb} = \delta_{ij}\delta_{ab}\Delta\varepsilon_{jb} + K_{ia,jb}, \tag{16}$$

$$B_{ia,jb} = K_{ia,bj}. \tag{17}$$

In these equations, i and j denote occupied orbitals and a and b denote virtual orbitals. **A** and **B** are defined here for a restricted approach, single excitation, and a functional without any fraction of Hartree-Fock exchange. For more general expressions, see Eq. 4.33 of Ref. [54]. For hybrid functionals, see Eq. 95-96 of Ref. [55].

In Eqs. (16)-(17),

$$\Delta\varepsilon_{jb} = \varepsilon_b - \varepsilon_j \tag{18}$$

is the difference between the KS energies of the orbitals and

$$K_{ia,jb} = \left(ia \mid jb\right) + \left(ia \mid f_{XC} \mid jb\right) \tag{19}$$

is given in terms of the two-electron integrals

$$\left(ia \mid jb\right) = \iint d\mathbf{r}d\mathbf{r}'\psi_i\left(\mathbf{r}\right)\psi_a\left(\mathbf{r}\right)\left(\mathbf{r}-\mathbf{r}'\right)^{-1}\psi_j\left(\mathbf{r}'\right)\psi_b\left(\mathbf{r}'\right) \tag{20}$$

$$\left(ia \mid f_{XC} \mid jb\right) = \iint d\mathbf{r}d\mathbf{r}'\psi_i\left(\mathbf{r}\right)\psi_a\left(\mathbf{r}\right)f_{XC}\psi_j\left(\mathbf{r}'\right)\psi_b\left(\mathbf{r}'\right) \tag{21}$$

for real KS orbitals ψ_k and within the adiabatic local density approximation (ALDA) [54]:

$$f_{XC} = \frac{\delta^2 E_{XC}}{\delta\rho\left(\mathbf{r}\right)\delta\rho\left(\mathbf{r}'\right)}, \tag{22}$$

where E_{XC} is the exchange-correlation energy.

If f_{XC} is neglected, the time-dependent Hartree-Fock (also known as the random phase approximation, RPA) is recovered [55]. If **B** = 0, we have the Tamm-Dancoff approximation (TDA) [55], which has been often used for surface hopping (see Section 4). Another approximation also often used in SH/DFT is the time-dependent density-functional-based tight binding (TD-DFTB) [56]. TD-DFTB is based on a second-order expansion of the KS total energy with respect to charge-density fluctuations, followed by a time-dependent linear-response procedure, where the transition densities $\psi_i\psi_a$ in the coupling matrix $K_{ia,jb}$ (Eqs. (19)-(21)) are approximated by atom-centered contributions [57].

To understand the next DFT methods for computing excitation energies and to also have a better insight in the meaning of the TDDFT solutions, we may explicitly check the structure of the TDDFT energies for a simple case of one occupied orbital p and two virtual orbitals r and s (Figure 1). For this minimal system, the eigenvalue problem in Eq. (14) can be written as

$$\begin{bmatrix} \Omega_{pr,pr} & \Omega_{pr,ps} \\ \Omega_{ps,pr} & \Omega_{ps,ps} \end{bmatrix} \begin{bmatrix} F_1 \\ F_2 \end{bmatrix} = \omega^2 \begin{bmatrix} F_1 \\ F_2 \end{bmatrix}. \tag{23}$$

The eigenvalues of this Hermitian problem are

$$\omega_{2,1}^2 = \left(\frac{\Omega_{pr,pr} + \Omega_{ps,ps}}{2} \right) \pm \sqrt{ \left(\frac{\Omega_{pr,pr} - \Omega_{ps,ps}}{2} \right)^2 + \Omega_{pr,ps}^2 }. \tag{24}$$

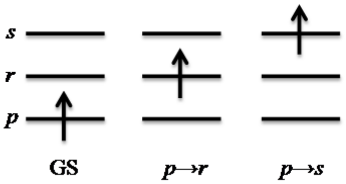

Figure 1. Schematic illustration of a reduced system with one occupied and two virtual orbitals. The ground state (GS) determinant can give origin to two single excitations.

If the nondiagonal terms of **Ω** are null (which occur when $K_{pr,ps} = K_{ps,pr} = 0$, see Eq. (26)), the excitations energies are simply

$$\omega_1 = \Omega_{pr,pr}^{1/2} \quad \omega_2 = \Omega_{ps,ps}^{1/2}, \tag{25}$$

implying that the energy of each sate is associated to an unique singly-excited determinant (for instance, $p \rightarrow r$) and independent from the remaining determinants.

The matrix elements of $\mathbf{\Omega}$ can be explicitly written as (see Eq. 4.33 of Ref.[54])

$$\Omega_{ia,jb} = \delta_{ij}\delta_{ab}\Delta\varepsilon_{jb}^{2} + 2\sqrt{\Delta\varepsilon_{ia}}K_{ia,jb}\sqrt{\Delta\varepsilon_{jb}}. \qquad (26)$$

With Eq. (26), the lowest excitation energy in Eq. (25) becomes

$$\omega_1 = \sqrt{\Delta\varepsilon_{pr}^{2} + 2\Delta\varepsilon_{pr}K_{pr,pr}}. \qquad (27)$$

(An equivalent equation holds for ω_2 due to $p \rightarrow s$ excitation.) If $K_{pr,pr} \ll \Delta\varepsilon_{pr}$, the excitation energy can be approximated by

$$\omega_1 \approx \Delta\varepsilon_{pr} + K_{pr,pr} \qquad (28)$$

This result corresponds to the excitation energy computed with density functional perturbation theory to the first order [58] and it is also directly obtained with TDA ($\mathbf{B} = 0$).

If $K_{pr,pr}$ is completely neglected, the excitation energy is given simply by the bare energy gap between orbitals

$$\omega_1 \approx \Delta\varepsilon_{pr} = \varepsilon_r - \varepsilon_p. \qquad (29)$$

corresponding to the zeroth order of the perturbative expansion [59].

One realistic situation where $K_{pr,pr}$ is near zero occurs in charge-transfer states. In such cases, ψ_p and ψ_r are localized in different parts of the molecules with little overlap. The excitation energy reduces to Eq. (29), which does not have the expected 1/R Coulomb attraction term, rendering the well known underestimation of the charge-transfer excitation energies [55].

The LR-TDDFT excitation energies given by Eq. (14) are derived by an analytic treatment of the poles of the dynamic polarizability of KS orbitals dynamically perturbed by an external field [54-55]. We have seen that LR-TDDFT improves the bare KS energy gap, Eq. (29), through two kinds of corrections. First, with diagonal terms that shift the energy of the uncoupled single excitation, Eq. (28), and, second, with nondiagonal terms, which bring contributions from all other single excitations in the KS orbital space, Eq. (24) [60].

A series of methods based on independent propagation of non-interacting orbitals through the time-dependent KS equation have been proposed to be used in connection to surface hopping [61-64]. In such methods, derived aiming at large systems with high density of states, the excited states are computed from single determinants or spin-adapted single configurations using KS orbitals, with energies given by the bare KS gaps. Eq. (29) is a particular case for an excited state represented by a singly-excited determinant. For more general cases, see Eq. 20 of

Ref.[61]. Throughout this paper, we refer to this class of methods for determining DFT excitation energies as single-determinant Kohn-Sham (SDKS).

A two-determinants DFT excitation method, the restricted open-shell Kohn-Sham (ROKS) by Frank and co-authors [65], was often employed in the earliest investigations of SH/DFT [66-68]. In that approximation, the ground state is taken as the usual closed-shell KS determinant, while the first excited state is represented by a spin-adapted singly-excited singlet configuration. The two determinants forming the configuration are formed from excited-state KS orbitals, which are obtained by optimizing an *ad hoc* energy functional designed to represent the singlet-triplet split in a two-electrons/two-orbitals configuration. Other formulations of restricted open-shell Kohn-Sham formalism have also been proposed in Refs. [69-71], but as far as we know, they have not been used in surface hopping simulations.

3.2 Nonadiabatic couplings in DFT

Nonadiabatic couplings between different electronic states are needed for propagation of surface hopping dynamics. While analytical energy gradients for excited states computed with TDDFT are well established [72] and implemented in diverse computational-chemistry programs, analytical nonadiabatic couplings are still mostly unavailable.

The theoretical background for computation of these couplings has been established by Chernyak and Mukamel [73] and, alternatively, by Baer [51]. Hu and co-workers have further developed the Chernyak-Mukamel approach for computation of first-order nonadiabatic coupling vectors between the ground state and the first excited state [74-76]. Send and Furche have shown that the previous result neglects molecular orbitals derivatives [77]. Their own derivation including such terms, but still limited to couplings between the ground and the first excited states, is implemented in Turbomole [78].

Due to the lack of analytical couplings between excited states in standard quantum-chemistry programs, finite-difference couplings have been largely used in surface hopping [32-34]. They are usually based on the approach proposed by Hammes-Schiffer and Tully [31], who showed that the couplings can be written in terms of wavefunction overlaps between sequential time steps during the dynamics (see Eq.(7)).

A particular problem to use TDDFT with this approach is the lack of an explicit wavefunction for the electronic states. A common solution has been to take the Casida's Ansatz for the state assignment [54] as an approximation to the wavefunctions. In this case, the ground and excited-state wavefunctions are given (for a local functional) by

$$\Psi_0 = \left|KS\right\rangle, \tag{30}$$

$$\Psi_L = \sum_{j,b} \sqrt{\frac{\Delta\varepsilon_{jb}}{\omega_L}} F_L^{jb} \left|jb\right\rangle, \tag{31}$$

$\left|KS\right\rangle$ is the ground-state KS determinant and $\left|jb\right\rangle$ is the determinant with a single excitation from j to b. With these wavefunctions, which are analogous to a CIS expansion, the coupling terms σ_{LM} can be evaluated according to Eq. (7) in terms of atomic orbital overlap integrals [33]. Although the validity of the Casida's Ansatz for computation of couplings approach still needs to be extensively tested, it has been shown that TDDFT dynamics computed with these couplings compares well with dynamics based on CASSCF [79] and MRCI [80].

Eq. (31) forms non-orthogonal set, which can have consequences for the evaluation of the couplings. Werner et al. [81] recommended the use the linear-response coefficients without the square-root term in Eq. (31) as the CIS coefficients, which forms a orthogonal set within TDA. An alternative solution is to orthogonalize the approximate wavefunctions given by Eq. (31) before computing the couplings. In practical terms, far from conical intersections with the ground state, either of these approximations provides similar dynamical pictures. In some cases, negative excitation energies are obtained (see Section 3.3), consequently the wavefunctions are complex and imaginary couplings may be obtained. In such situations, as we discuss later, it is not recommendable to continue the SH/TDDFT propagation.

The Casida wavefunctions given in Eqs. (30) and (31) have been employed by Tavernelli and co-workers to derive analytical nonadiabatic coupling vectors between the ground and the first excited states [82] and also between excited states [83]. They are given by

$$\boldsymbol{\tau}_{0L} = \sum_{ia} \sqrt{\frac{\Delta\varepsilon_{ia}}{\omega_L}} F_L^{ia} \left\langle \psi_i \right| \nabla_{\mathbf{R}} H_{KS} \left| \psi_a \right\rangle, \tag{32}$$

$$\begin{aligned}\boldsymbol{\tau}_{LM} &= \sum_{iab} \sqrt{\frac{\Delta\varepsilon_{ia}}{\omega_L}} \sqrt{\frac{\Delta\varepsilon_{ib}}{\omega_M}} F_L^{ia\dagger} F_M^{ib} \left\langle \psi_a \right| \nabla_{\mathbf{R}} H_{KS} \left| \psi_b \right\rangle \\ &- \sum_{ija} \sqrt{\frac{\Delta\varepsilon_{ia}}{\omega_L}} \sqrt{\frac{\Delta\varepsilon_{ja}}{\omega_M}} F_L^{ia\dagger} F_M^{ja} \left\langle \psi_i \right| \nabla_{\mathbf{R}} H_{KS} \left| \psi_j \right\rangle.\end{aligned} \tag{33}$$

(As in the previous section, ψ_k corresponds to the molecular orbitals, i,j runs over occupied orbitals, and a,b over virtual orbitals.)

In Ref. [84] it is shown that τ_{0L} in Eq. (32) is equivalent to the analytical coupling vector derived by Hu *et al*. in Ref. [74], but, also as the Hu *et al*.'s result, it does not fully agree with Chernyak-Mukamel [73]. Ou et al. [36] have pointed out that in the formalism leading to Eqs. (32) and (33), only the KS Fock matrix is differentiated, omitting the full coupling that is induced by the second derivative of the exchange-correlation functionals. Still working with a CIS expansion based on TDA amplitudes, these authors have derived nonadiabatic coupling vectors (including excited-excited terms) fully consistent with Chernyak-Mukamel [36].

Apart of their limitations, Eqs. (32) and (33) are general results, which are still valid by replacing the operator $\nabla_{\mathbf{R}} H_{KS}$ by any single-body operator $\hat{O}$ [83], as, for example, the electronic dipole operator, to obtain the transition dipole moment $\boldsymbol{\mu}_{LM}$.

Recently, spin-orbit coupling elements [85] were also derived based on the Casida wavefunctions, opening the possibility to perform surface hopping between surfaces with different multiplicities within the TDDFT approach. The coupling between singlet and triplet states, for instance, is given by

$$H_{ST}^{SO} = \sum_{ia\rho, jb\rho'} \sqrt{\frac{\Delta\varepsilon_{ia\rho}}{\omega_S}} F_S^{ia\rho} \sqrt{\frac{\Delta\varepsilon_{jb\rho'}}{\omega_T}} F_T^{jb\rho'} \langle ia_S | H^{SO} | jb_T \rangle, \tag{34}$$

where ρ and ρ' are spin indexes. In Ref. [85], H^{SO} is approximated by the 1-electron Breit-Pauli operator [86]. The computation of the 2-electron operator is discussed by Chiodo and Russo in Refs. [87-88].

In Ref. [89], the computation of Dyson orbitals based on Casida wavefunctions is discussed. These Dyson orbitals were used to evaluate photoionizaton cross-sections during the dynamics and to simulate time-dependent photoelectron imaging spectra.

In SDKS methods, the computation of the couplings is largely simplified by the singe-determinant approximation. As shown in Eq. 21 of Ref. [61], the couplings in such cases are reduced to derivatives of KS orbitals, which can be inexpensively computed by finite differences during the dynamics propagation.

For a discussion about the computation of the nonadiabatic couplings in ROKS, see Ref. [90]. For a discussion about computation of these couplings with REKS see Ref. [91].

3.3 Critical appraisal

One of the main challenges in excited-sate dynamics simulations is that trajectories span large regions of the configuration space. Thus, the electronic structure method used to compute energies, energy gradients, couplings, and other properties should be able to deal with a large variety of electronic densities induced by different conformations.

A good deal of the problem comes from a bad description of the ground state (see Figure 2). Strictly speaking, DFT should be valid even at the crossing seam between the ground and the first excited state, as the Hohenberg-Kohn theorems [92] can be generalized to degenerate ground states [93-94]. However, the KS formulation of DFT needs to fulfill two basic conditions [95]: 1) the reference state should be a single-determinant state to compute exchange energy and 2) the correlation hole should be reasonably described by homogenous (or weakly inhomogeneous) electron gas to compute the correlation energy. In diverse cases–as, for instance, in biradicals species, where nondynamic electron correlation plays a strong role–one of or both conditions are not satisfied, rendering a bad description of the ground state and, consequently, of the excited-states based upon. In particular, the methods for computing excitation energies discussed in Section 3.1 have in common the assumption that the ground state can be described by a single KS determinant. (For a conceptual discussion of nondynamic electron correlation in DFT, see Ref. [95]. For a discussion about conical intersection in DFT, see Ref. [96])

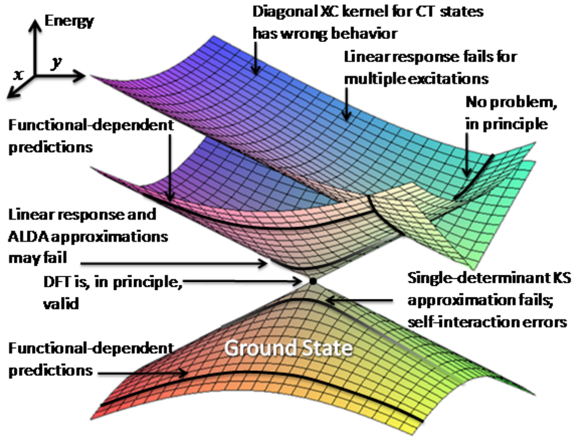

Figure 2. Illustration of the main problems with DFT and TDDFT occurring in different regions of the ground- and excited-state surfaces.

The development of a density functional theory including nondynamic (or "strong") electron correlation–which Becke designated as the "last frontier" in DFT [97]–has been pursued by many groups following different approaches. Among those approaches, we may cite the use of restricted open-shell ground-state representations [98], configuration ensembles with fractional occupations [91, 99-101], configuration interaction [102-103], multiconfigurational DFT

[104], hybrid multiconfiguration/(TD)DFT [105-106], and spin-unrestricted broken-symmetry (UBS) [107] approaches. Unfortunately, analytical energy gradients are not available for most of these methods, which rules out their use in surface hopping dynamics.

All the troubles caused by nondynamic electron correlation are rather restricted to the crossing between the ground and the first excited state. In the case of crossing between excited states, however, if each of these states is well represented by single excitations from a well-behaved ground state, the description of the crossing does not present further problems.

SH/DFT has other potential problems (Figure 2) besides nondynamical electron correlation. First, the results are deeply dependent on the functional. Second, double and higher excitations are not properly described by LR-TDDFT. Third, diffuse and charge-transfer states may be poorly described by conventional functionals. All these problems though are not exclusive of dynamics simulations and are also part of routine investigations of excited states based on DFT. As such, they are addressed in the same way, by systematic test of functionals, methodological comparisons, and use of range-separated functionals.

To illustrate the current situation of excited state description for SH/DFT, we show in Figure 3 the potential-energy surfaces for the S_1 state and for the S_1/S_0 gap of ethylene along two important reaction coordinates, H_2CCH_2-torsion (θ) and CCH_2-pyramidalization (φ). All other coordinates are kept at their ground-state values optimized at the same level as used for energy calculations. These surfaces were computed with several different DFT-based methods and with *ab-initio* MR-CISD, which is taken as the reference method. With the exception of the DFT-MRCI [102], computed with the SV(P) basis set [108], all other DFT-based surfaces were computed with the 6-31G* basis set [109]. LC-BLYP [110-112] was computed with $\mu = 0.2\ a_0^{-1}$ [113]. TD-DFTB was based on analytic expressions for the matrix elements [114]. MR-CISD was based on a small (2 electrons, 2 orbitals)-space [115] with the aug-cc-pVTZ basis set [116] assigned to C and cc-pVDZ assigned to H.

Ethylene S_1 surface is a specially challenging problem, starting from 1) the adequate computation of the excitation into the V state [6], then 2) the description of the right topography of the state, which includes a crossing with the Z state near the twisted structure and a conical intersection at twisted-pyramidalized geometries [115], to finally 3) the dynamics evolution itself, which has motivated a long debate between theorists and experimentalists [117-119]. In fact, Levine et al. [120] have used maps similar to those in Figure 3 (but computed for stretched CC distances) to discuss the qualitative deficiencies in the excited-state description provided by TDDFT.

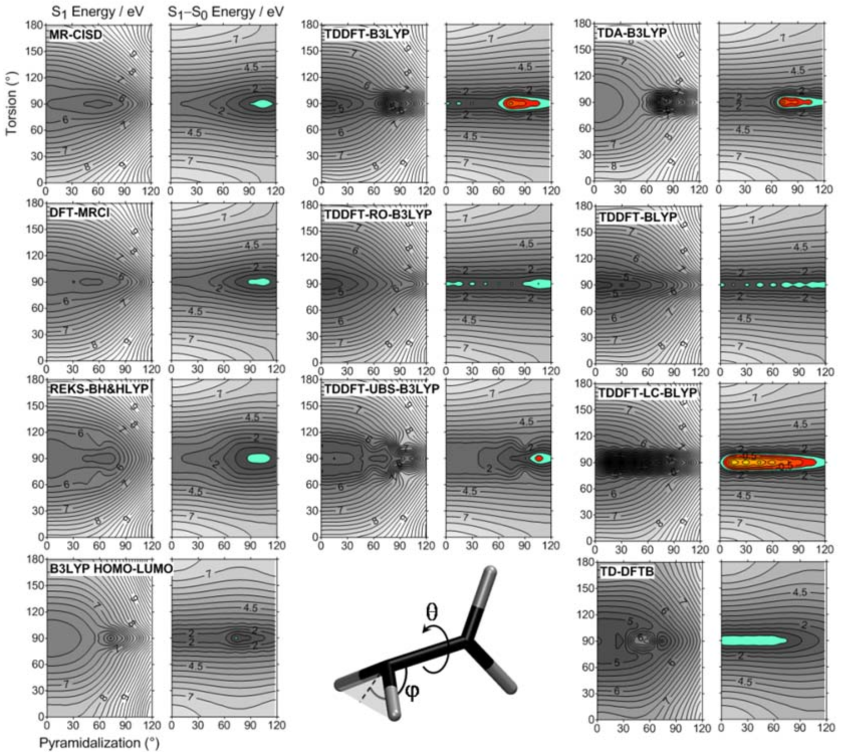

Figure 3. S$_1$ and S$_1$–S$_0$ potential-energy surfaces of ethylene computed with diverse methods. Green regions indicate the crossing seam. Red/orange regions are negative energy gaps. In the illustration, ethylene has θ = 90° and φ = 45°.

The MR-CISD result in Figure 3 has two main features that dominate the topography and the dynamics in the S$_1$ state: 1) there is a S$_1$ minimum near θ = 90° and φ = 60° and 2) there is a conical intersection at θ = 90° and φ = 110°. Among all tested methods, the only ones that were able to reproduce both features are the DFT-MRCI [102] and REKS [91, 99, 101], which makes clear the importance of having a multiconfigurational description of the ground state. TDDFT-UBS, which is usually considered a good alternative for qualitatively recovering nondynamic electron correlation near a degeneracy [71] can describe reasonably well the conical intersection, but the topography along the θ = 90° line shows diverse spurious minima.

Spurious minima were also observed in TDDFT and TDA with B3LYP [121-122]. The minimum is at qualitatively wrong position at TDDFT-B3LYP with restricted open shell (TDDFT-RO). The same happens for TDDFT-BLYP. TDA can qualitatively predict the conical intersection ($\theta = 90°$, $\varphi > 70°$). Somewhat surprisingly, the simple HOMO-LUMO gap is the only other method predicting a twisted-pyramidalized conical intersection (at $\theta = 90°$, $\varphi = 70°$). All other methods wrongly predict an extended S_1/S_0 seam along the $\theta = 90°$ line, starting from $\varphi = 0°$.

A disturbing feature that can be observed in TDDFT-B3LYP, TDDFT-UBS-B3LYP, TDA-B3LYP, and TDDFT-LC-BLYP is that the excitation may become negative near the crossing seam. This is not an exclusive problem of DFT-based methods, but it can be observed in other single-reference methods as well, like coupled cluster either with equation-of-motion or linear-response approaches.

As discussed in Ref. [123], near the degeneracy, self-interaction errors may cause the HOMO to be less stable than the LUMO, leading to imaginary excitation energies in TDDFT (see Eq. (27)). This does not happen at TDA because the excitation energy is given by terms like in Eq. (28). This feature has been claimed to represent an improved stability of the TDA-based dynamics in comparison to that based on TDDFT [123]. Nevertheless, as we can see in the negative gap regions in Figure 3, both methods are still unstable near the degeneracy. These negative excitations are clearly due to the mixing with the other singly-excited determinants, which can be avoided neither in TDDFT nor in TDA.

In SDKS methods, the excitation energies are given by the bare KS gaps [61]. In the case of the ethylene, we can see in Figure 3 that the bare KS energy (given by the HOMO-LUMO gap and neglecting double excitations near the twisted structure) gives an adequate representation of the S_1 state and of the S_1-S_0 gap. This good behavior, however, should not be taken for granted. Maitra [60], in a critical discussion of these approximation in the context of surface hopping, showed that the bare KS energies may be far from adiabatic and closer to diabatic energies.

Ethylene is admittedly a too harsh case for DFT-based methods, as its dynamics is deeply controlled by coordinates involved in the nonadiabatic events. SH/DFT methods have been developed to deal with large molecular systems and in these cases the dynamics may evolve in the configurational space spanning regions relatively far from any muticonfigurational ground state. Under such situation, the excited-state dynamics involving a large manifold of excited states can be well simulated with DFT-based methods.

Take, for instance, the schematic dynamics illustrated in Figure 4-top. The dynamics starts at a high excited state (here, the second state to simplify the picture). Using a multireference method like MRCI, we would observe a relaxation to the first excited state (a), then oscillation around the minimum of this state (b). From this minimum, the molecule can eventually fluoresce to the ground state (c) or cross a barrier (d) to reach a conical intersection, from where it relaxes to the ground state minimum (e).

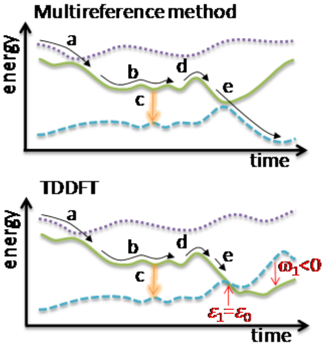

Figure 4. Schematic comparison of a trajectory computed with surface hopping based on multireference method (top) and on TDDFT (bottom).

In principle, SH/TDDFT can adequately describe most of this process (Figure 4-bottom). The relaxation through the manifold of excited states (a) can be described if these states are dominated by single excitations from a well-behaved ground state and if the functional allows to describe special features like charge-transfer states. The oscillation around the excited minimum (b) is also not a problem, at least if this minimum is not on the top of a multiconfigurational ground state. Neither the radiative process (c) nor the barrier crossing (d) presents any special problems, apart from functional dependencies. Even the relaxation until near the crossing with the ground state (e) can in principle be described. In fact, all this process may be better described with TDDFT and other correlated single-reference methods like the algebraic diagrammatic construction to the second order (ADC(2) [124-125]), than with an uncorrelated multiconfigurational method like CASSCF [35]. The real problem starts very close to the state crossing (usually for energy gaps smaller than 0.1 eV), where the convergence of the KS equations tends to fail and even if convergence is achieved, regions with negative excitation energies may be reached. Besides that, as discussed by Levine *et al.*[120], the lack of nonadiabatic interactions between the ground and the excited states may lead in some cases to the wrong dimensionality of the intersection seam with the ground state. (See Ref. [126] for a comparative discussion of the shape of the crossing seam computed with different methods.)

Although diverse groups working with SH/DFT choose to compute hops to the ground state, it is our opinion that the results obtained from this procedure are not reliable. We have adopted as strategy to stop the dynamics simulations as soon as a certain energy-gap threshold is reached, usually 0.15 eV (see, for instance, Ref. [127]). This last time step is then taken as an estimate of the time for internal conversion to the ground state. This strategy, which we apply not only for TDDFT, but also for ADC(2) [35, 128], allows the computation of excited-state lifetimes and the early split of population between different reaction channels, but unfortunately it does not provide enough information for computation of reaction yields in the ground state.

4 Surface-hopping/DFT implementations

One of the reasons of the popularity of the surface hopping method is that its implementation is straightforward. This has given rise to several home-made private codes to simulate SH/DFT [62-63, 81, 129]. There are also few general programs of public access (either commercial or non-commercial) with SH/DFT capability, including Newton-X [130-131], PYXAID [61, 132], Turbomole [78], and CPMD [133].

The main difference among the several implementations of SH/DFT is exactly which DFT method is being used for computing the electronic-structure quantities. The main features of the most common implementations are summarized in Table 1.

Table 1. Survey of diverse implementations of SH/DFT. Excited states can be computed with linear response time-dependent (LR-TD) theory, single determinant KS (SDKS), or restricted open shell KS (ROKS); Single (SS) or multiple (MS) excited states can be included; states can be restricted to single (SE) or multiple (ME) excitations; propagation can be done in terms of Gaussian functions (GF) or plane waves (PW).

DFT excitations	Number of states	Excitation level	Basis type	Refs.	Public implementation
LR-TDDFT	MS	SE	GF	[32]	Newton-X
LR-TDDFT	SS	SE	GF	[77]	Turbomole
LR-TD-DFTB	MS	SE	GF	[137]	
TDA	MS	SE	GF	[38]	Newton-X
TDA	MS	SE	PW	[34, 83]	CPMD
ROKS	SS	SE	PW	[68]	CPMD
SDKS	MS	ME	GF	[63]	
SDKS	MS	ME	GF	[62]	
SDKS	MS	ME	PW	[61, 134]	PYXAID

The most computationally efficient implementation of SH/DFT available is based on SDKS approximations [134], as that implemented in the PYXAID program using plane waves. Variants of this method have also been developed by Fischer, Handt, and Schmidt [50, 62, 135] using Gaussian functions, by Gao and co-workers using DFTB KS orbitals [63], and by Shenvi, Roy, and Tully based on a model Hamiltonian parameterized by DFT data [64, 136]. SDKS has been used to investigate diverse problems, especially in condensed matter (see Section 5). Besides the computational efficiency granted by the single-determinant approximation, Shenvi and co-workers [64] have pointed out that while in TDDFT the electronic Hilbert space must be truncated to include only a relatively small number of states, this restriction does not apply to SDKS, being a big advantage for the treatment of systems with large density of states. Moreover, SDKS also allows the inclusion of double and higher excitations [61]. On the down side, the bare KS energy gaps may not only strongly deviate from the exact energies, but also provide a poor approximation for adiabatic surfaces [60].

Still aiming at maximum computational optimization, Prezhdo and co-workers have also introduced the so called “classical path approximation” (CPA) in PYXAID [61]. The CPA implies that the nuclear dynamics is supposed to evolve independently of the electrons, driven by kinetic effects. In practical terms, it means that the nuclear dynamics is propagated in the ground state and then it is used to compute the nonadiabatic electronic events in the excited states using either the fewest switches surface hopping or one of the other surface hopping algorithms developed by Prezhdo group [132]. The CPA may be especially inadequate for systems undergoing significant chemical changes like photofragmentation and chemical reactions.

Another efficient implementation of SH/DFT is based on ROKS and was developed by Doltsinis and Marx [138]. The spin-adapted wavefunctions and the KS orbitals optimized for the excited-state density should in principle be an improvement over the SDKS. SH/ROKS, however, is limited to a single excited state, which is a very strong limitation for most of realistic problems. Such approach is implemented in the CPMD program.

SH/LR-TDDFT has been pioneered by Tavernelli and Rothlisberger [34] and by Mitrić and Bonačić-Koutecký [81]. Linear response should provide a better description of the excited-state surfaces than single determinant and ROKS approaches, at higher computational costs naturally (see Section 3.1). TDDFT is also not limited to a single surface as ROKS, but it cannot describe multiple excitations. In the framework of linear response, surface hopping dynamics has been investigated with TDDFT, TDA, and TD-DFTB (see Section 5). In CPMD program, this approach is implemented based on plane waves, while in Newton-X, it is implemented based on localized basis. It is also implemented in Turbomole, but limited to couplings between the ground state and the first excited state. Ehrenfest dynamics [139], another related semiclassical nonadiabatic dynamics method, can be performed with TDDFT using the Octopus program [140].

In the case of Newton-X, the coefficients c_L to compute the hopping probabilities (Eq. (10)) can be obtained either by integrating Eq. (4) or by using the local diabatization method (Eq, (8)). The program also allows the computation of surface hopping through interfaces with different programs (Turbomole, Gaussian

[141], Columbus [142-143], Gamess [144]) and using different methods (TDA, TDDFT, ADC(2), CC2, CASSCF, MRCI), making it specially convenient for comparative analysis.

5 Case studies

There are a large number of molecular systems investigated with SH/DFT. This section does not aim at providing a comprehensive review of them, but to point out the main classes of problems in different fields, from where the reader can search for more information.

SH/DFT has been developed mainly aiming at the treatment of large systems, for which wavefunction-based methods are computationally too expensive. It is possible, however, to find a series of investigations for photoreactions of small molecules (see Table 2), which has been useful to gauge the quality of these simulations. $CH_2NH_2^+$, for instance, has been used as a test case of SH/TDA [34, 79] and SH/SDKS [145]. In both cases, qualitative agreement with surface SH/CASSCF [146] is observed. We should note, however, that this agreement may be accidental, as $CH_2NH_2^+$ is a very small system with only two relevant excited states, a single dominant reaction path, and lifetime shorter than 100 fs. More impressive is the semi-quantitative agreement observed between SH/TDDFT [80] and SH/MRCI [147] for pyrrole. In this case, TDDFT dynamics with 10 excited states has successfully predicted the excited-state lifetime and the split of population among several reaction paths.

A more applied class of systems investigated with SH/DFT excitations involves photoinduced proton transfer and photoinduced isomerization in medium-sized molecules. A typical example of such class is azobenzene, which has been studied with SH/ROKS [148] and SH/SDKS [149]. Dynamics based on both provide a good description of the cis-trans izomerization of azobenzene in the gas phase in comparison to other semiempirical and *ab-initio* wavefunction-based surface hopping simulations [150-154]. Azobenzene has been chosen by a number of groups, including ours, as a standard test-case for methods. We should consider, however, that this molecule may not be challenging enough to be a good test case. After S_1 excitation, azobenzene evolves adiabatically until finding the intersection to the ground state, approaching the crossing seam along torsional coordinates. These features imply that neither nonadiabatic effects between excited states nor the dimensionality of the crossing seam can be really tested with this system. On the other hand, azobenzene is an excellent system to probe the topography of S_1 and the S_1/S_0 coupling strength, which can be done through simulations of excited-state lifetime and isomerization yield.

Table 2. Survey of case studies with SH/DFT.

System	Method	Ref.	System	Method	Ref.
Basic processes in small molecules			*Systems of biological interest*		
Pyrrole, imidazole, furan	TDDFT	[80, 89, 155]	Diphenyldibenzofulvene	SDKS	[63]
Pyrazine	TDDFT	[81, 156]	Riboflavin	TDDFT	[157]
Pyrrole	ROKS	[158]	Kynurenine	TDDFT	[129]
CH_2=NH	ROKS	[68]	Adenine	TDDFT	[35, 159]
CH_2=NH_2^+	TDA, SDKS	[79, 145]	Adenine gas and in water	TDDFTB	[137]
CH_2Cl-CF_3	TDDFT	[160]	Guanine, cytosine, uracil,	ROKS	[66, 161-163]
Oxyrane	TDA	[123]	Guanine-cytosine pairs	ROKS	[164]
Indole in water	TDDFT	[165]	Protonated tryptophan	TDA	[166]
$O(^3P)+C_2H_2$ (ISC)	ΔUDFT	[167]	Acetylphenylalaninylamide	TDDFT	[168]
Photoinduced proton transfer, isomerization			*Systems of interest for materials sciences, surfaces*		
Hydroxyquinoline-NH_3	TDA	[169]	Carbon nanotubes	SDKS	[170-171]
Methylformamide dimer	TDDFT	[127]	Graphene	SDKS	[172]
Bridged azobenzene	ROKS	[173]	$Cd_{33}Se_{33}$, $Si_{29}H_{24}$ (quantum dot)	SDKS	[23, 145]
Azobenzene gas and in water	ROKS	[148]	NO/Au(111)	SDKS	[64, 136]
Azobenzene, Stilbene	SDKS	[149]	Pentacene crystal	SDKS	[61]
Diphenydibenzofulvene	SDKS	[63]	Pentacene/C_{60}	SDKS	[174]
Catalysis			*Reviews*		
$Cr(CO)_6$	TDDFT	[175]	Nonadiabatic phenomena		[8, 126, 176]
Ru (II) trisbipyridine in water	TDA	[177]	Surface hopping		[11, 139, 178]
Chromophore-TiO_2	SDKS	[134]	Dynamics/TDDFT		[20, 179]
Water splitting on GaN	SDKS	[180]	DFT excited states		[54-55, 181]

One of the main problems with SH/DFT is the deep dependence on the chosen functional. This can be illustrated with an example that we have recently investigated, the excited-state dynamics of N-methylformamide dimer (NMF) [127]. These simulations showed that NMF dimers are protected against photodissociation by a proton-transfer mechanism. The excited-state proton transfer occurs according the Sobolewski-Domcke mechanism [182], where an electron is transferred before and then followed by the proton (see Fig. 5). For properly describing the charge-transfer state, SH/TDDFT was done with the range-separated LC-BLYP functional [110-112]. The range-separation parameter was fixed at $\mu = 0.2\ a_0^{-1}$, a value based on a non-empirical parameterization [113]. Our tests with diverse values of μ showed that the ratio between dissociation and proton transfer was deeply dependent on this parameter. Not surprisingly, larger values favored dissociation by under-stabilizing the charge-transfer state. (In Gaussian program [141], for instance, the default value of m is $0.47\ a_0^{-1}$.) Lower values favored proton transfer for the opposite reason.

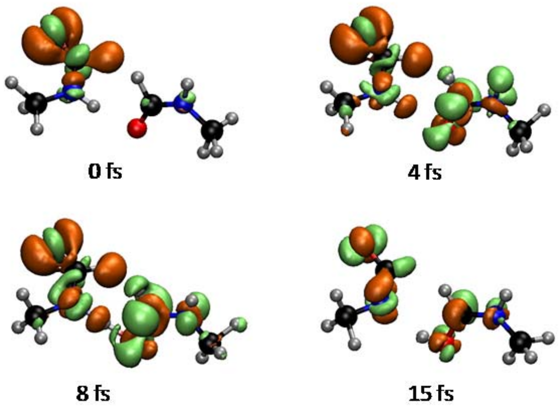

Figure 5. Evolution of the (S_1-S_0) electron density difference during a single surface-hopping trajectory of N-methylformamide dimer computed with TDDFT with LC-BLYP ($\mu = 0.2\ a_0^{-1}$). Green (orange) indicates electron acceptor (donor) regions. Based on data from Ref. [127].

Diverse systems of biological interest have also been investigated with SH/DFT (see Table 2). In this class, a challenging case has been the description of purine nucleobases. An indication of the problem was already in the earliest simulations of 9Me-keto guanine with SH/ROKS [161-162], whose trajectories did not reveal any conical intersection with the ground state. At that point, the internal conversion of guanine was attributed to an enhanced nonadiabatic coupling promoted by out-of-plane vibrations. Later, SH/TD-DFTB [137] predicted an excited-state lifetime of 11 ps for adenine gas, ten times longer than the experimental result. The deviation was then attributed to the distribution of initial energies. More recently, systematic investigations of adenine gas with SH/TDDFT with several functionals once more led to very long excited-state lifetimes [35, 159]. These results are conveniently plotted in Figure 6 in terms of the S_0 population 1 ps after photoexcitation. Even the most optimistic SH/TDDFT simulation at the limit of the error bar is inferior to 40%, while the experimental result reaches 68%. The root of the problem seems to be connected by an overstabilization of the ground state energy along planar distortions in comparison to nonplanar distortions. This unbalanced ground state profile leads to a wrong description of the excited-state minimum [159].

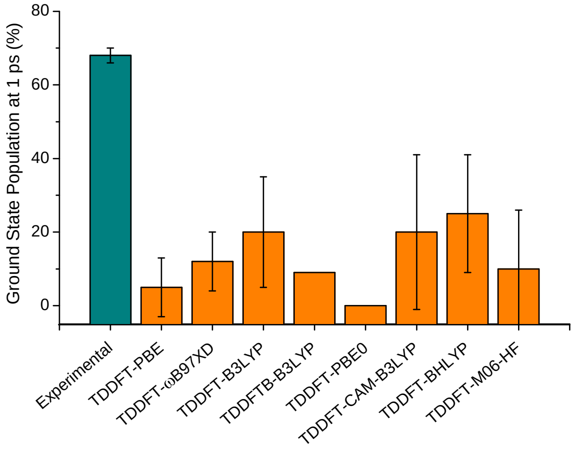

Figure 6. Ground state population of adenine gas 1 ps after photoexcitation according to the experiment [183] and to surface hopping based on diverse LR-TDDFT simulations. TDDFT data from Refs. [35, 159]. TDDFTB from Ref. [137] (supposing simple exponential decay). Sampling error of the simulations for 90% confidence level.

SH/SDKS has allowed to stretch the limits of the simulations to much beyond it can currently be done with TDDFT or wavefunction-based methods. In particular, it has allowed to investigate large organic chromophores [63], adsorbance of molecules on metal [64, 136] and semiconductor [134, 180] surfaces, Auger dynamics in quantum dots [23], carbon nanostructures [170, 172], and organic crystals [61, 174].

An interesting example in this class of systems related to condensed matter and materials science is the recently published simulations for a P3HT/carbon-nanotube heterojunction [171]. Organic heterojunctions have been intensively explored for the development of organic photovoltaics based on photoinduced electron transfer [184-185]. P3HT (poly(3-hexylthiophene)) is a standard organic polymer used as chromophore and electron donor [186], while carbon nanotubes (CNT) are electron-acceptor materials with enhanced charge-transport properties [187]. Notwithstand the limitations of DFT to approach this type of system [188], dynamics with SH/SDKS predicts that there is a strong asymmetry between the electron and hole transports in P3HT/CNT interface (Figure 7). While photoexcitation of P3HT leads to an electron transfer within 100 fs, the hole transfer takes much longer, occurring in the few picoseconds scale.

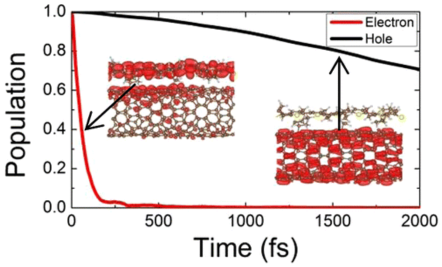

Figure 7. Decay of the population of the electron and hole donor states in a P3HT (donor) – nanotube (acceptor) interface. Reprinted with permission from Ref. [171]. Copyright 2014 American Chemical Society.

6 Conclusions

In the last decade, surface hopping dynamics has become an essential tool for the investigation of nonadiabatic processes in diverse fields, providing fundamental information to interpret data from time-resolved spectroscopy, to explain photochemical process, and to predict new properties with potential technological applications. Motivated by the advances in computational capabilities and algorithms, such simulations are under constant pressure to address always larger and more complex systems. The development of SH/DFT has opened possibilities to go much beyond wavefunction *ab-initio* methods could achieve.

In most of implementations reported in the literature so far, DFT excitations used for surface hopping are obtained either from linear-response time-dependent theory or from bare KS gaps. Currently, we observe a large effort from different research groups to generalize the methods for different kinds of nonadiabatic interactions, to provide better theoretical foundations, and to improve the hopping algorithms. The availability of SH/DFT in few public computational-chemistry softwares has also helped to popularize the method.

SH/DFT very successfully expanded the range of systems that can be approached for nonadiabatic dynamics investigations. We should, however, be aware that many methodological restrictions remain and must still be properly addressed. Such restrictions involve intrinsic limitations in the semi-classical local approach for nonadiabatic dynamics, in the sampling of statistical ensembles, and more fundamentally in the quality of the DFT excited-state predictions. In particular, the multireference character of regions of energy crossing between the excited and the ground states is still a challenge waiting for better solutions than those provides so far.

Acknowledgments

We would like to thank Dr. Michael Filatov for gently providing the REKS data for Figure 3 and also Dr. W. Arbelo-González, Dr. Fazzi, Dr. G. Rodrigues, and Dr. T. Very for helpful discussions.

References

[1] Winter NOC, Graf NK, Leutwyler S, Hattig C (2013) Phys Chem Chem Phys 15: 6623.

[2] Silva-Junior MR, Thiel W (2010) J Chem Theory Comput 6: 1546.

[3] Silva-Junior MR, Schreiber M, Sauer SPA, Thiel W (2010) J Chem Phys 133: 174318.

[4] Schreiber M, Silva-Junior MR, Sauer SPA, Thiel W (2008) J Chem Phys 128: 134110.

[5] Silva-Junior MR, Schreiber M, Sauer SPA, Thiel W (2008) J Chem Phys 129: 104103.

[6] Wu W, Zhang H, Braïda B, Shaik S, Hiberty P (2014) Theor Chem Acc 133: 1.

[7] Dreuw A, Weisman JL, Head-Gordon M (2003) J Chem Phys 119: 2943.

[8] Yonehara T, Hanasaki K, Takatsuka K (2011) Chem Rev 112: 499.

[9] Yarkony DR (2011) Chem Rev 112: 481.

[10] Worth GA, Cederbaum LS (2004) Annu Rev Phys Chem 55: 127.

[11] Barbatti M (2011) WIREs: Comp Mol Sci 1: 620.

[12] Nelson T, Fernandez-Alberti S, Roitberg AE, Tretiak S (2013) J Chem Phys 138: 224111.

[13] Zheng J, Meana-Pañeda R, Truhlar DG (2014) J Phys Chem Lett 5: 2039.

[14] Nelson T, Fernandez-Alberti S, Chernyak V, Roitberg AE, Tretiak S (2012) J Chem Phys 136: 054108.

[15] Akimov AV, Prezhdo OV (2014) Phys Rev Lett 113: 153003.

[16] Gorshkov VN, Tretiak S, Mozyrsky D (2013) Nat Commun 4.

[17] Kelly A, van Zon R, Schofield J, Kapral R (2012) J Chem Phys 136: 084101.

[18] Nikitin EE (1968) In: Hartmann H, Heidberg J, Heydtmann H, Kohlmaier GH (eds) Chemische Elementarprozesse. Springer-Verlag, Berlin

[19] Tully JC, Preston RK (1971) J Chem Phys 55: 562.

[20] Curchod BFE, Rothlisberger U, Tavernelli I (2013) ChemPhysChem 14: 1314.

[21] Akimov AV, Neukirch AJ, Prezhdo OV (2013) Chem Rev 113: 4496.

[22] Fabiano E, Keal TW, Thiel W (2008) Chem Phys 349: 334.

[23] Wang L, Trivedi D, Prezhdo OV (2014) J Chem Theory Comput: doi:10.1021/ct5003835.

[24] Fabiano E, Groenhof G, Thiel W (2008) Chem Phys 351: 111.

[25] Kammerer CF, Lasser C (2008) J Chem Phys 128: 144102.

[26] Lasser C, Swart T (2008) J Chem Phys 129: 034302.

[27] Zhu C, Nakamura H, Nobusada K (2000) Phys Chem Chem Phys 2: 557.

[28] Tully JC (1990) J Chem Phys 93: 1061.

[29] Blais NC, Truhlar DG (1983) J Chem Phys 79: 1334.

[30] Jaeger HM, Fischer S, Prezhdo OV (2012) J Chem Phys 137: 22A545.

[31] Hammes-Schiffer S, Tully JC (1994) J Chem Phys 101: 4657.

[32] Mitrić R, Werner U, Bonačić-Koutecký V (2008) J Chem Phys 129: 164118.

[33] Pittner J, Lischka H, Barbatti M (2009) Chem Phys 356: 147.

[34] Tapavicza E, Tavernelli I, Rothlisberger U (2007) Phys Rev Lett 98: 023001.

[35] Plasser F, Crespo-Otero R, Pederzoli M, Pittner J, Lischka H, Barbatti M (2014) J Chem Theory Comput 10: 1395.

[36] Ou Q, Fatehi S, Alguire E, Shao Y, Subotnik JE (2014) J Chem Phys 141: 024114.

[37] Granucci G, Persico M, Toniolo A (2001) J Chem Phys 114: 10608.

[38] Plasser F, Granucci G, Pittner J, Barbatti M, Persico M, Lischka H (2012) J Chem Phys 137: 22A514.

[39] Wang L, Prezhdo OV (2014) J Phys Chem Lett 5: 713.

[40] Schwartz BJ, Bittner ER, Prezhdo OV, Rossky PJ (1996) J Chem Phys 104: 5942.

[41] Zhu CY, Nangia S, Jasper AW, Truhlar DG (2004) J Chem Phys 121: 7658.

[42] Akimov AV, Long R, Prezhdo OV (2014) J Chem Phys 140: 194107.

[43] Granucci G, Persico M (2007) J Chem Phys 126: 134114.

[44] Granucci G, Persico M, Zoccante A (2010) J Chem Phys 133: 134111.

[45] Bajo JJ, González-Vázquez J, Sola IR, Santamaria J, Richter M, Marquetand P, González L (2011) J Phys Chem A 116: 2800.

[46] Granucci G, Persico M, Spighi G (2012) J Chem Phys 137: 22A501.

[47] Jones GA, Acocella A, Zerbetto F (2008) J Phys Chem A 112: 9650.

[48] Mitric R, Petersen J, Bonacic-Koutecky V (2009) Phys Rev A 79: 053416.
[49] Tavernelli I, Curchod BFE, Rothlisberger U (2010) Phys Rev A 81: 052508.
[50] Fischer M, Handt J, Schmidt R (2014) Phys Rev A 90: 012527.
[51] Baer R (2002) Chem Phys Lett 364: 75.
[52] Lopata K, Govind N (2011) J Chem Theory Comput 7: 1344.
[53] Dobson JF, Bunner MJ, Gross EKU (1997) Phys Rev Lett 79: 1905.
[54] Casida M (1995) In: Chong D (ed) Recent advances in density functional methods, Part I. World Scientific, Singapore p 155
[55] Dreuw A, Head-Gordon M (2005) Chem Rev 105: 4009.
[56] Elstner M, Porezag D, Jungnickel G, Elsner J, Haugk M, Frauenheim T, Suhai S, Seifert G (1998) Phys Rev B 58: 7260.
[57] Niehaus TA, Suhai S, Della Sala F, Lugli P, Elstner M, Seifert G, Frauenheim T (2001) Phys Rev B 63: 085108.
[58] Gonze X, Scheffler M (1999) Phys Rev Lett 82: 4416.
[59] Görling A (1996) Phys Rev A 54: 3912.
[60] Maitra NT (2006) J Chem Phys 125: 014110.
[61] Akimov AV, Prezhdo OV (2013) J Chem Theory Comput 9: 4959.
[62] Fischer M, Handt J, Schmidt R (2014) Phys Rev A 90: 012525.
[63] Gao X, Peng Q, Niu Y, Wang D, Shuai Z (2012) Phys Chem Chem Phys 14: 14207.
[64] Shenvi N, Roy S, Tully JC (2009) J Chem Phys 130: 174107.
[65] Frank I, Hutter J, Marx D, Parrinello M (1998) J Chem Phys 108: 4060.
[66] Doltsinis NL, Markwick PRL, Nieber H, Langer H (2008) In: Shukla MK, Leszczynski J (eds) Radiation Induced Molecular Phenomena in Nucleic Acids. Springer Netherlands p 265
[67] Röhrig UF, Guidoni L, Laio A, Frank I, Rothlisberger U (2004) J Am Chem Soc 126: 15328.
[68] Doltsinis NL, Marx D (2002) Phys Rev Lett 88: 166402.
[69] Filatov M, Shaik S (1998) Chem Phys Lett 288: 689.
[70] Okazaki I, Sato F, Yoshihiro T, Ueno T, Kashiwagi H (1998) J Mol Struct THEOCHEM 451: 109.
[71] Gräfenstein J, Kraka E, Cremer D (1998) Chem Phys Lett 288: 593.
[72] Furche F, Ahlrichs R (2002) J Chem Phys 117: 7433.
[73] Chernyak V, Mukamel S (2000) J Chem Phys 112: 3572.
[74] Hu C, Hirai H, Sugino O (2007) J Chem Phys 127: 064103.
[75] Hu C, Sugino O, Tateyama Y (2009) J Chem Phys 131: 114101.
[76] Hu C, Sugino O, Watanabe K (2014) J Chem Phys 140: 054106.
[77] Send R, Furche F (2010) J Chem Phys 132: 044107.
[78] Ahlrichs R, Bär M, Häser M, Horn H, Kölmel C (1989) Chem Phys Lett 162: 165.
[79] Tavernelli I, Tapavicza E, Rothlisberger U (2009) J Mol Struct THEOCHEM 914: 22.

[80] Barbatti M, Pittner J, Pederzoli M, Werner U, Mitrić R, Bonačić-Koutecký V, Lischka H (2010) Chem Phys 375: 26.
[81] Werner U, Mitrić R, Suzuki T, Bonačić-Koutecký V (2008) Chem Phys 349: 319.
[82] Tavernelli I, Tapavicza E, Rothlisberger U (2009) J Chem Phys 130: 124107.
[83] Tavernelli I, Curchod BFE, Laktionov A, Rothlisberger U (2010) J Chem Phys 133: 194104.
[84] Tavernelli I, Curchod BFE, Rothlisberger U (2009) J Chem Phys 131: 196101.
[85] Franco de Carvalho F, Curchod BFE, Penfold TJ, Tavernelli I (2014) J Chem Phys 140.
[86] Marian CM (2012) Wiley Interdisciplinary Reviews: Computational Molecular Science 2: 187.
[87] Chiodo S, Russo N (2008) J Comput Chem 29: 912.
[88] Chiodo SG, Russo N (2010) Chem Phys Lett 490: 90.
[89] Humeniuk A, Wohlgemuth M, Suzuki T, Mitrić R (2013) J Chem Phys 139: 134104.
[90] Billeter SR, Curioni A (2005) J Chem Phys 122: 034105.
[91] Filatov M (2014) Top Curr Chem: in press.
[92] Hohenberg P, Kohn W (1964) Phys Rev 136: B864.
[93] Gross EKU, Oliveira LN, Kohn W (1988) Phys Rev A 37: 2805.
[94] Katriel J, Zahariev F, Burke K (2001) Int J Quantum Chem 85: 432.
[95] Cremer D (2001) Mol Phys 99: 1899.
[96] Huix-Rotllant M, Nikiforov A, Thiel W, Filatov M (2014) Top Curr Chem: in press.
[97] Becke AD (2014) J Chem Phys 140: 18A301.
[98] Cremer D (2013) WIREs: Comp Mol Sci 3: 482.
[99] Filatov M, Shaik S (1999) Chem Phys Lett 304: 429.
[100] Gross EKU, Oliveira LN, Kohn W (1988) Phys Rev A 37: 2809.
[101] Filatov M (2014) WIREs: Comp Mol Sci: doi:10.1002/wcms.1209.
[102] Grimme S, Waletzke M (1999) J Chem Phys 111: 5645.
[103] Beck EV, Stahlberg EA, Burggraf LW, Blaudeau J-P (2008) Chem Phys 349: 158.
[104] Kurzweil Y, Lawler KV, Head-Gordon M (2009) Mol Phys 107: 2103.
[105] Sharkas K, Savin A, Jensen HJA, Toulouse J (2012) J Chem Phys 137: 044104.
[106] Fromager E, Knecht S, Jensen HJA (2013) J Chem Phys 138.
[107] Gräfenstein J, Kraka E, Filatov M, Cremer D (2002) Int J Mol Sci 3: 360.
[108] Weigend F, Ahlrichs R (2005) Phys Chem Chem Phys 7: 3297.
[109] Hehre WJ, Ditchfield. R, Pople JA (1972) J Chem Phys 56: 2257.
[110] Iikura H, Tsuneda T, Yanai T, Hirao K (2001) J Chem Phys 115: 3540.
[111] Becke AD (1988) Phys Rev A 38: 3098.
[112] Lee C, Yang W, Parr RG (1988) Phys Rev B 37: 785.

[113] Minami T, Nakano M, Castet F (2011) J Phys Chem Lett 2: 1725.

[114] Zheng G, Witek HA, Bobadova-Parvanova P, Irle S, Musaev DG, Prabhakar R, Morokuma K, Lundberg M, Elstner M, Köhler C, Frauenheim T (2007) J Chem Theory Comput 3: 1349.

[115] Barbatti M, Paier J, Lischka H (2004) J Chem Phys 121: 11614.

[116] Dunning TH (1989) J Chem Phys 90: 1007.

[117] Sellner B, Barbatti M, Müller T, Domcke W, Lischka H (2013) Mol Phys 111: 2439.

[118] Mori T, Glover WJ, Schuurman MS, Martinez TJ (2012) J Phys Chem A 116: 2808.

[119] Kosma K, Trushin SA, Fuss W, Schmid WE (2008) J Phys Chem A 112: 7514.

[120] Levine BG, Ko C, Quenneville J, Martínez TJ (2006) Mol Phys 104: 1039.

[121] Becke AD (1993) J Chem Phys 98: 5648.

[122] Stephens PJ, Devlin FJ, Chabalowski CF, Frisch MJ (1994) J Phys Chem 98: 11623.

[123] Tapavicza E, Tavernelli I, Rothlisberger U, Filippi C, Casida ME (2008) J Chem Phys 129: 124108.

[124] Hättig C (2005) Adv Quantum Chem 50: 37.

[125] Schirmer J (1982) Phys Rev A 26: 2395.

[126] Gozem S, Melaccio F, Valentini A, Filatov M, Huix-Rotllant M, Ferré N, Frutos LM, Angeli C, Krylov AI, Granovsky AA, Lindh R, Olivucci M (2014) J Chem Theory Comput 10: 3074.

[127] Crespo-Otero R, Mardykov A, Sanchez-Garcia E, Sander W, Barbatti M (2014) Phys Chem Chem Phys 16: 18877.

[128] Barbatti M (2014) J Am Chem Soc 136: 10246.

[129] Tuna D, Došlić N, Mališ M, Sobolewski AL, Domcke W (2014) J Phys Chem B: doi:10.1021/jp501782v.

[130] Barbatti M, Granucci G, Ruckenbauer M, Plasser F, Crespo-Otero R, Pittner J, Persico M, Lischka H (2013) NEWTON-X: a package for Newtonian dynamics close to the crossing seam: www.newtonx.org.

[131] Barbatti M, Ruckenbauer M, Plasser F, Pittner J, Granucci G, Persico M, Lischka H (2014) WIREs: Comp Mol Sci 4: 26.

[132] Akimov AV, Prezhdo OV (2014) J Chem Theory Comput 10: 789.

[133] CPMD: www.cpmd.org.

[134] Craig CF, Duncan WR, Prezhdo OV (2005) Phys Rev Lett 95: 163001.

[135] Fischer M, Handt J, Schmidt R (2014) Phys Rev A 90: 012526.

[136] Shenvi N, Tully JC (2012) Faraday Discuss 157: 325.

[137] Mitrić R, Werner U, Wohlgemuth M, Seifert G, Bonačić-Koutecký V (2009) J Phys Chem A 113: 12700.

[138] Doltsinis NL (2002) In: Grotendorst J, Marx D, Muramatsu A (eds) Quantum Simulations of Complex Many-Body Systems: From Theory to Algorithms. John von Neumann Institute for Computing, Julich

[139] Tully JC (1998) Faraday Discuss 110: 407.
[140] Castro A, Appel H, Oliveira M, Rozzi CA, Andrade X, Lorenzen F, Marques MAL, Gross EKU, Rubio A (2006) Phys Status Solidi B 243: 2465.
[141] Frisch MJ, Trucks GW, Schlegel HB, Scuseria GE, Robb MA, Cheeseman JR, Scalmani G, Barone V, Mennucci B, Petersson GA, Nakatsuji H, Caricato M, Li X, Hratchian HP, Izmaylov AF, Bloino J, Zheng G, Sonnenberg JL, Hada M, Ehara M, Toyota K, Fukuda R, Hasegawa J, Ishida M, Nakajima T, Honda Y, Kitao O, Nakai H, Vreven T, Montgomery J, J. A., Peralta JE, Ogliaro F, Bearpark M, Heyd JJ, Brothers E, Kudin KN, Staroverov VN, Kobayashi R, Normand J, Raghavachari K, Rendell A, Burant JC, Iyengar SS, Tomasi J, Cossi M, Rega N, Millam NJ, Klene M, Knox JE, Cross JB, Bakken V, Adamo C, Jaramillo J, Gomperts R, Stratmann RE, Yazyev O, Austin AJ, Cammi R, Pomelli C, Ochterski JW, Martin RL, Morokuma K, Zakrzewski VG, Voth GA, Salvador P, Dannenberg JJ, Dapprich S, Daniels AD, Farkas Ö, Foresman JB, Ortiz JV, Cioslowski J, Fox DJ (2013) Gaussian 09, Revision D.01. Gaussian, Inc., Wallingford CT.
[142] Lischka H, Müller T, Szalay PG, Shavitt I, Pitzer RM, Shepard R (2011) WIREs: Comp Mol Sci 1: 191.
[143] Lischka H, Shepard R, Shavitt I, Pitzer RM, Dallos M, Müller T, Szalay PG, Brown FB, Ahlrichs R, Böhm HJ, Chang A, Comeau DC, Gdanitz R, Dachsel H, Ehrhardt C, Ernzerhof M, Höchtl P, Irle S, Kedziora G, Kovar T, Parasuk V, Pepper MJM, Scharf P, Schiffer H, Schindler M, Schüler M, Seth M, Stahlberg EA, Zhao J-G, Yabushita S, Zhang Z, Barbatti M, Matsika S, Schuurmann M, Yarkony DR, Brozell SR, Beck EV, Blaudeau J-P, Ruckenbauer M, Sellner B, Plasser F, Szymczak JJ (2012) COLUMBUS, an ab initio electronic structure program, release 7.0: www.univie.ac.at/columbus.
[144] Gordon MS, Schmidt MW (2005) In: Dykstra CE, Frenking G, Kim KS, Scuseria GE (eds) Theory and Applications of Computational Chemistry the first forty years. Elsevier, Amsterdam p 1167
[145] Fischer SA, Habenicht BF, Madrid AB, Duncan WR, Prezhdo OV (2011) J Chem Phys 134.
[146] Barbatti M, Aquino AJA, Lischka H (2006) Mol Phys 104: 1053.
[147] Vazdar M, Eckert-Maksic M, Barbatti M, Lischka H (2009) Mol Phys 107: 845
[148] Bockmann M, Doltsinis NL, Marx D (2010) J Phys Chem A 114: 745.
[149] Neukirch AJ, Shamberger LC, Abad E, Haycock BJ, Wang H, Ortega J, Prezhdo OV, Lewis JP (2013) J Chem Theory Comput 10: 14.
[150] Weingart O, Lan Z, Koslowski A, Thiel W (2011) J Phys Chem Lett 2: 1506.
[151] Pederzoli M, Pittner J, Barbatti M, Lischka H (2011) J Phys Chem A 115: 11136.
[152] Carstensen O, Sielk J, Schonborn JB, Granucci G, Hartke B (2010) J Chem Phys 133: 124305.

[153] Ootani Y, Satoh K, Nakayama A, Noro T, Taketsugu T (2009) J Chem Phys 131: 194306.

[154] Gao A-H, Li B, Zhang P-Y, Liu J (2014) Comput Theor Chem 1031: 13.

[155] Crespo-Otero R, Barbatti M, Yu H, Evans NL, Ullrich S (2011) ChemPhysChem 12: 3365.

[156] Tomasello G, Humeniuk A, Mitrić R (2014) J Phys Chem A 118: 8437.

[157] Klaumunzer B, Kroner D, Lischka H, Saalfrank P (2012) Phys Chem Chem Phys 14: 8693.

[158] Frank I, Damianos K (2007) J Chem Phys 126: 125105.

[159] Barbatti M, Lan Z, Crespo-Otero R, Szymczak JJ, Lischka H, Thiel W (2012) J Chem Phys 137: 22A503.

[160] Pereira Rodrigues G, Ventura E, do Monte SA, Barbatti M (2014) J Phys Chem A: doi:10.1021/jp507681g.

[161] Langer H, Doltsinis NL (2004) Phys Chem Chem Phys 6: 2742.

[162] Langer H, Doltsinis NL, Marx D (2005) ChemPhysChem 6: 1734.

[163] Nieber H, Doltsinis NL (2008) Chem Phys 347: 405.

[164] Markwick PRL, Doltsinis NL, Schlitter J (2007) J Chem Phys 126: 045104.

[165] Wohlgemuth M, Bonačić-Koutecký V, Mitrić R (2011) J Chem Phys 135.

[166] Mercier SR, Boyarkin OV, Kamariotis A, Guglielmi M, Tavernelli I, Cascella M, Rothlisberger U, Rizzo TR (2006) J Am Chem Soc 128: 16938.

[167] Hu W, Lendvay G, Maiti B, Schatz GC (2008) J Phys Chem A 112: 2093.

[168] Mališ M, Loquais Y, Gloaguen E, Biswal HS, Piuzzi F, Tardivel B, Brenner V, Broquier M, Jouvet C, Mons M, Došlić N, Ljubić I (2012) J Am Chem Soc 134: 20340.

[169] Guglielmi M, Tavernelli I, Rothlisberger U (2009) Phys Chem Chem Phys 11: 4549.

[170] Habenicht BF, Prezhdo OV (2008) Phys Rev Lett 100: 197402.

[171] Long R, Prezhdo OV (2014) Nano Lett 14: 3335.

[172] Habenicht BF, Prezhdo OV (2009) J Phys Chem C 113: 14067.

[173] Böckmann M, Doltsinis NL, Marx D (2010) Angew Chem 122: 3454.

[174] Akimov AV, Prezhdo OV (2014) J Am Chem Soc 136: 1599.

[175] Crespo-Otero R, Barbatti M (2011) J Chem Phys 134: 164305.

[176] Garavelli M (2006) Theor Chem Acc 116: 87.

[177] Tavernelli I, Curchod BFE, Rothlisberger U (2011) Chem Phys 391: 101.

[178] Jasper AW, Zhu CY, Nangia S, Truhlar DG (2004) Faraday Discuss 127: 1.

[179] Casida M, Natarajan B, Deutsch T (2012) In: Marques MAL, Maitra NT, Nogueira FMS, Gross EKU, Rubio A (eds) Fundamentals of Time-Dependent Density Functional Theory. Springer Berlin Heidelberg p 279

[180] Akimov AV, Muckerman JT, Prezhdo OV (2013) J Am Chem Soc 135: 8682.

[181] Casida ME, Huix-Rotllant M (2012) Annu Rev Phys Chem 63: 287.
[182] Sobolewski AL, Domcke WG (2007) J Phys Chem A 111: 11725.
[183] Evans NL, Ullrich S (2010) J Phys Chem A 114: 11225.
[184] Mishra A, Bäuerle P (2012) Angew Chem Int Ed 51: 2020.
[185] Ameri T, Khoram P, Min J, Brabec CJ (2013) Adv Mater 25: 4245.
[186] Grancini G, Polli D, Fazzi D, Cabanillas-Gonzalez J, Cerullo G, Lanzani G (2011) J Phys Chem Lett 2: 1099.
[187] Veera S, Nismy NA, Adikaari AADT, Simon JH, Maxim S, Silva SRP (2011) Nanotechnology 22: 265607.
[188] Sen K, Crespo-Otero R, Weingart O, Thiel W, Barbatti M (2013) J Chem Theory Comput 9: 533.